

PAPER • OPEN ACCESS

## Predicting the peak structural displacement preventing pounding of buildings during earthquakes

To cite this article: S M Khatami *et al* 2021 *J. Phys.: Conf. Ser.* **2070** 012010

View the [article online](#) for updates and enhancements.

A promotional banner for the 241st ECS Meeting. The left side has a blue background with white and dark blue text. The right side features a photograph of the Science World geodesic dome in Vancouver, BC, Canada, with modern buildings in the background under a clear blue sky.

**ECS** The Electrochemical Society  
Advancing solid state & electrochemical science & technology

### 241st ECS Meeting

May 29 – June 2, 2022 Vancouver • BC • Canada  
Abstract submission deadline: Dec 3, 2021

Connect. Engage. Champion. Empower. Accelerate.  
**We move science forward**

 Submit your abstract

# Predicting the peak structural displacement preventing pounding of buildings during earthquakes

S M Khatami<sup>1</sup>, H Naderpour<sup>2</sup>, A Mortezaei<sup>3</sup>, S T. Tafreshi<sup>4</sup>, A Jakubczyk-Galczyńska<sup>5\*</sup>, R Jankowski<sup>5</sup>

<sup>1</sup> University of Applied Science and Technology, Center of Semnan Municipality, Semnan, Iran.

<sup>2</sup> Faculty of Civil Engineering, Semnan University, Semnan, Iran.

<sup>3</sup> Seismic Geotechnical and High Performance Concrete Research Centre, Civil Engineering Department, Semnan Branch, Islamic Azad University, Semnan, Iran  
Faculty of Civil Engineering, Semnan University, Semnan, Iran.

<sup>4</sup> Islamic Azad University, Central Tehran Branch, Civil Engineering Department, Tehran, Iran Faculty of Civil Engineering, Semnan University, Semnan, Iran.

<sup>5</sup> Gdańsk University of Technology, Faculty of Civil and Environmental Engineering, ul. Narutowicza 11/12, 80-233 Gdańsk, Poland

\* Corresponding author, e-mail: annjakub@pg.edu.pl

**Abstract.** The aim of the present paper is to verify the effectiveness of the artificial neural network (ANN) in predicting the peak lateral displacement of multi-story building during earthquakes, based on the peak ground acceleration (PGA) and building parameters. For the purpose of the study, the lumped-mass multi-degree-of-freedom structural model and different earthquake records have been considered. Firstly, values of stories mass and stories stiffness have been selected and building vibration period has been automatically calculated. The ANN algorithm has been used to determine the limitation of the peak lateral displacement of the multi-story building with different properties (height of stories, number of stories, mass of stories, stiffness of stories and building vibration period) exposed to earthquakes with various PGA. Then, the investigation has been focused on critical distance between two adjacent buildings so as to prevent their pounding during earthquakes. The proposed ANN has logically predicted the limitation of the peak lateral displacement for the five-story building with different properties. The results of the study clearly indicate that the algorithm is also capable to properly predict the peak lateral displacements for two buildings so as to prevent their pounding under different earthquakes. Subsequently, calculation of critical distance can also be optimized to save the land and provide the safety space between two adjacent buildings prone to seismic excitations.

## 1. Introduction

It is obviously seen that insufficient separation distance between buildings may provide serious damages due to collisions during earthquakes [1,2]. This phenomenon, called structural pounding, occurs when critical distance cannot cover relative movements of structures and large lateral displacements exceed the in-between separation gap [3-6]. In order to investigate pounding in buildings, many researchers have experimentally tested collisions between structures and structural models with real and unreal scales, and also, have numerically presented different equations to



Content from this work may be used under the terms of the [Creative Commons Attribution 3.0 licence](https://creativecommons.org/licenses/by/3.0/). Any further distribution of this work must maintain attribution to the author(s) and the title of the work, journal citation and DOI.



calculate impact damping ratio for evaluating pounding and separation distance (see, for example, [7-10]).

The sufficient separation distance preventing pounding between two adjacent buildings during earthquakes has been mathematically determined by various authors. On the other hand, the majority of building codes have suggested appropriate formulae to determine minimum gap for providing enough space in order to prevent building collisions (see [11-13]). For this challenge, the absolute sum method (ABS) and the sum of the squares of the modal response (SRSS) are usually used [11,12]:

$$S = \delta_i + \delta_j \quad (1)$$

$$S = \sqrt{\delta_i^2 + \delta_j^2} \quad (2)$$

where  $S$  is the gap size between buildings,  $\delta_i$  and  $\delta_j$  denote peak lateral displacement of buildings  $i$  and  $j$ , respectively. It should also be mentioned that some codes, considering structural height,  $h$ , recommend separation distance between buildings as follows [13]:

$$S = 0.05(h_i + h_j) \quad (3)$$

A number of researchers indicated that period of buildings and also, inherently structural damping coefficient must be considered in order to calculate separation distance as buildings show nonlinear behavior during seismic excitation (see, for example, [14-17]).

Different studies were focused on numerical methods to suggest equations based on building codes to provide separation distance between structures. They also considered damages due to pounding between buildings and indicated that the critical distance is the most important issue to study methods of preventing collisions during earthquakes. Naderpour et al. [7,8] studied a series of impacts to calculate impact damping ratio and estimate impact velocity based on the coefficient of restitution. Subsequently, they suggested an equation of impact damping ratio to calculate impact between two bodies and the effect of gap size to avoid collisions. Lopez-Garcia [9,10] focused deeply on separation distance and suggested some parameters to prevent pounding between structures. Kiureghian [14] suggested a new equation to calculate separation distance based on period and damping ratio of buildings. Jeng et al. [15] proposed the spectral difference method based on random vibration theory that considers the first mode approximation for displacements of elastic multi-story buildings. Filatrault et al. [18] improved the equation of separation distance by using effect of damping ratio. Penzien [19] also recommended calculating an effective period to use original period. Rahman et al. [20] studied mitigation measures for earthquake-induced structural pounding.

Therefore it is noticeable that the most important parameter in zone of building pounding is the lateral displacement, which can be decreased or controlled by different methods. Thus, the aim of the present paper is to predict the peak lateral structural displacement during different earthquakes based on the peak ground acceleration (PGA) and building vibration period. The artificial neural network (ANN) has been applied for this purpose. Using the discrete multi-degree-of-freedom numerical models of buildings, different cases have been studied (various stories mass, stories stiffness, building vibration period and earthquake records) so as to obtain the best strategy to predict peak lateral displacement for each model.

## 2. Different methods to calculate critical distance

In order to determine required separation distance between two buildings, various authors tested different methods. Separation distance depends on the peak lateral displacements, as shown in equations (1) and (2), which have to be calculated for each building in order to determine critical distance between adjacent structures. Jeng et al. [15] suggested a new equation, based on SRSS formula, which can be written as:

$$S = \sqrt{\delta_i^2 + \delta_j^2 - 2\rho_{op}\delta_i\delta_j} \quad (4)$$

where  $\rho_{op}$  is the cross-correlation coefficient determined as [15]:

$$\rho_{op} = \frac{8\sqrt{\zeta_i \zeta_j} \left( \zeta_j + \zeta_i \frac{T_j}{T_i} \right) \left( \frac{T_j}{T_i} \right)^{\frac{3}{2}}}{\left( 1 - \left( \frac{T_j}{T_i} \right)^2 \right)^2 + 4\zeta_i \zeta_j \left( 1 + \left( \frac{T_j}{T_i} \right)^2 \right) \frac{T_j}{T_i} + 4(\zeta_i^2 + \zeta_j^2) \left( \frac{T_j}{T_i} \right)^2} \quad (5)$$

where  $T_i, T_j$  are the elastic vibration periods and  $\zeta_i, \zeta_j$  are the damping ratios of buildings. Moreover, Penzien [19] proposed the following equations for the nonlinear vibration period,  $T_{i-non}$ , and the nonlinear damping ratio,  $\zeta_{i-non}$ , of building  $i$ :

$$T_{i-non} = T_i \sqrt{\phi_i} \quad (6)$$

$$\zeta_{i-non} = \zeta_i + \omega_i \quad (7)$$

where  $\phi_i$  and  $\omega_i$  are demonstrated by formulae:

$$\phi_i = \frac{\mu_i}{\gamma + \alpha_i(\mu_i - \gamma)} \quad (8)$$

$$\omega_i = \frac{2}{\pi} \frac{(\mu_i - \gamma)(1 - \alpha_i)}{\mu_i(\gamma + \alpha_i(\mu_i - \gamma))} \quad (9)$$

where  $\mu_i$  is the displacement ductility,  $\gamma$  is a parameter with recommended value equal to 0.65 and  $\alpha_i$  is the ratio of ultimate stiffness to the initial one. Substitution of subscript  $i$  by  $j$  gives the corresponding expressions for building  $j$ .

Based on equations (6) and (7), Jeng et al. [15] suggested a new equation to calculate the nonlinear values of structural period and damping ratio:

$$\phi_i = (1 + 0.18(\mu_i - 1)) \quad (10)$$

$$\omega_i = 0.16(\mu_i - 1)^{0.9} \quad (11)$$

Finally, Naderpour et al. [21] numerically generated a new equation for the cross-correlation coefficient, based on a cyclic process, by using periods of both buildings, and investigated the accuracy of the formula:

$$\rho_{op} = \frac{T_j}{T_i} - 10.5(T_j - T_i) \quad (12)$$

Khatami et al. [22] also suggested the equation to calculate the nonlinear effective period of building as equal to:

$$T_n = T_i(1 + \alpha_i) \rightarrow \alpha_i = \eta_i(\mu^{0.385} - 1) \quad (13)$$

In this equation,  $\mu$  denotes the displacement ductility and  $0.93 \leq \eta \leq 0.97$ . It can be clearly seen from the above equations that calculation of sufficient gap size between adjacent structures in order to prevent building pounding depends significantly on the peak lateral structural displacements during the earthquake.

### 3. Application of ANN

There are different methods which can be used to predict various types of phenomena, including decision trees and risk analysis (see [23]), statistics and random algorithms (for example [24]) or artificial intelligence and machine learning (see [25-28]). The process of prediction of the peak lateral

displacement of building under earthquake excitation is presented in this paper using the ANN and the investigation is conducted to confirm the accuracy of the method.

Many researchers (see [29-31] for example) have confirmed that the use of ANN is an effective tool to predict different phenomena. In order to create an algorithm predicting the peak lateral structural displacement, it is necessary to build an artificial neuron. The process of building network consists of three basic steps: learning, validation and testing. The first step is to create a database necessary to start building of the algorithm. For this purpose, the properties of the structural model are firstly presented. Then, numerical study, focused on collecting samples to the network, is shown. In the last step, the created networks are presented.

### 3.1. Properties of structural model

Investigation of the best prediction of the peak lateral displacement has been carried out by using the lumped-mass multi-degree-of-freedom model of five-story building (see Figure 1). It has been assumed that the model is able to capture vibrations in all directions due to seismic excitation; but two directions (X and Y) have been estimated to have similar responses. Hence, X direction has been assumed to be the main one and the results for different cases have been directly compared with each other.

In the study, numerical analyses have been carried out so as to investigate the peak lateral displacement and predict the optimum separation distance between two adjacent buildings. The height of each story of building has been assumed to be 3.00 m and the plan of the structure is considered to be square. Different stories masses, from 15000 kg to 55000 kg with step of 1000 kg, and stories stiffness, from  $0.1 \times 10^6$  N/m to  $5 \times 10^6$  N/m with step of  $5 \times 10^4$  N/m, have been assumed for each model. The numerical analysis has been conducted for six earthquake records, i.e. El Centro (1940), Parkfield (1966), San Fernando (1971), Loma Prieta (1989), Kobe (1995) and Kocaeli (1999) - see Table 1. For this challenge, values of stories mass and stories stiffness have been selected and building vibration period has been automatically calculated. Then, the model has been analyzed and the peak lateral displacement has been depicted.

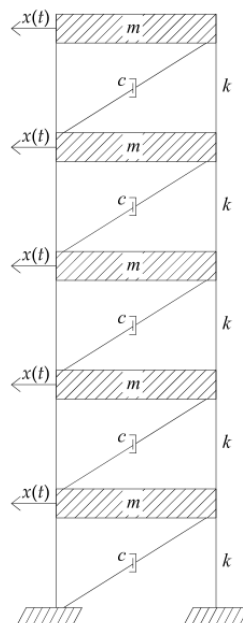


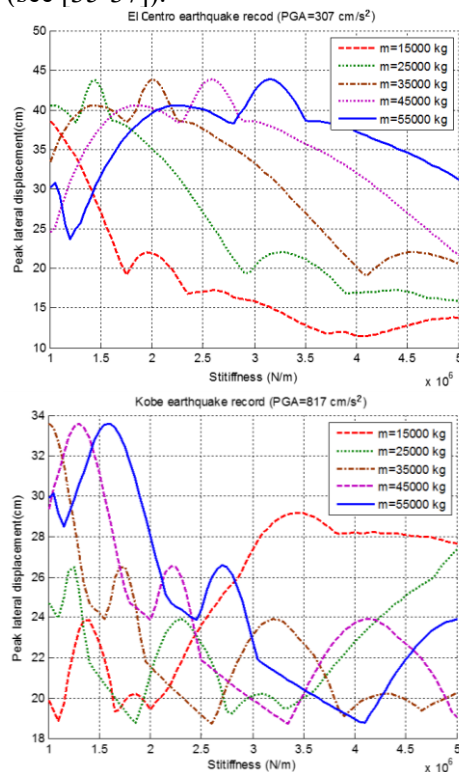
**Fig. 1** Schematic model of five-story building used in the investigation.

**Table 1** Ground motion records used in the analysis.

Earthquake	Date	Magnitude	Station	Component	PGA ( $\text{cm/s}^2$ )
Kocaeli	17.08.1999	7.6	Sakarya	EW	369.28
Kobe	17.01.1995	7.2	JMA	NS	817.82
Parkfield	28.06.1966	6.2	Jennings (CG)	NS	462.00
El Centro	18.05.1940	6.9	El Centro	NS	307.00
San Fernando	09.02.1971	6.6	Pacoima Dam	N16°W	1202.62
Loma Prieta	17.10.1989	6.9	Rinaldi Re St.	EW	631.00

### 3.2. Numerical study

For the purpose of the study, a five-story lumped-mass model with different stories mass and stories stiffness and also six mentioned earthquake records have been considered. Linear elastic numerical models have been used in the analyses. Previous studies have shown that inelastic behavior can significantly increase the lateral displacement responses of low-rise (short-period) buildings, whereas, for tall (long-period) buildings, inelastic behavior can reduce the lateral displacement responses only up to some extent (see [32-34] for example). In this study, soil-structure-interaction effects have been neglected. The inherent damping of the building has been modeled using 5% Rayleigh damping. It should be added that, for the case of inelastic buildings, modified versions of Rayleigh damping have been proposed in the literature (see [35-37]).



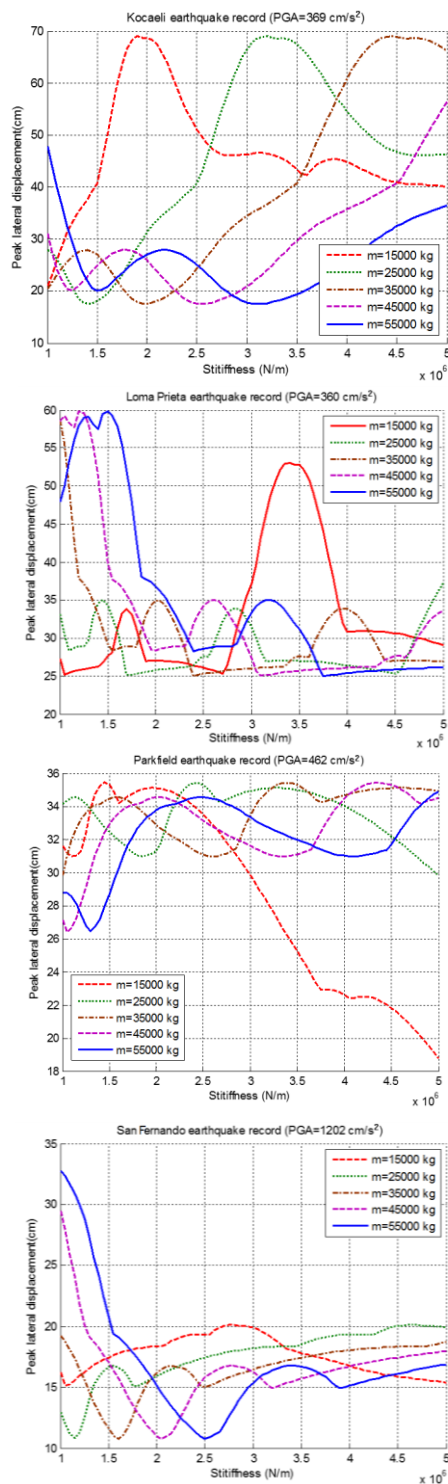


**Fig. 2** Peak lateral displacements for different models of buildings under various earthquakes.

Firstly, the structural model with various stories mass and stories stiffness has been analyzed under six earthquake records and the top story peak lateral displacement of each model has been determined. The examples of the results are shown in Figure 2 and Table 2. As it could be expected, different properties of the model (i.e. stories mass and stories stiffness), under a specified earthquake record, show substantially different values of the peak lateral displacement. In particular, Figure 2 and Table 2

indicate that the peak lateral displacement of the model under the El Centro earthquake record is equal to 43.89 cm while the building vibration period is 2.91 s. Furthermore, the peak lateral displacement of the model for the Kobe earthquake record is 33.76 cm while the building vibration period is 4.11 s. Investigation of the peak lateral displacement of the model for the Kocaeli earthquake record has showed a value of 69.2 cm when the building vibration period is equal to 1.95 s. The peak lateral displacement of the model under the Kocaeli earthquake record is the highest one among all used earthquake records (69.2 cm) while it has the lowest building vibration period comparing to other models. The peak lateral displacement of the model analyzed under the Loma Prieta earthquake record is 59.9 cm and also the building vibration period is 4.22 s. Values of building vibration period of 4.23 s and the peak lateral displacement of 59.9 cm have been obtained for the Parkfield earthquake record.

**Table 2** Maximum peak lateral displacements for different models of buildings under various earthquakes.

Earthquake record	PGA (cm/s <sup>2</sup> )	Story mass (kg)	Story stiffness (N/m)	Building vibration period (s)	Maximum peak lateral displacement (cm)
El Centro	307	15000	$0.89 \times 10^6$	2.91	43.89
		25000	$1.45 \times 10^6$		
		35000	$2.00 \times 10^6$		
		45000	$2.61 \times 10^6$		
		55000	$3.15 \times 10^6$		
Kobe	817	15000	$0.42 \times 10^6$	4.11	33.76
		25000	$0.7 \times 10^6$		
		35000	$1 \times 10^6$		
		45000	$1.3 \times 10^6$		
		55000	$1.6 \times 10^6$		
Kocaeli	369	15000	$1.9 \times 10^6$	1.96	69.2
		25000	$3.2 \times 10^6$		
		35000	$4.45 \times 10^6$		
		45000	$5.62 \times 10^6$		
		55000	$7.05 \times 10^6$		
Loma Prieta	631	15000	$0.4 \times 10^6$	4.22	59.9
		25000	$0.7 \times 10^6$		
		35000	$0.9 \times 10^6$		
		45000	$1.2 \times 10^6$		
		55000	$1.5 \times 10^6$		
Parkfield	462	15000	$1.5 \times 10^6$	2.23	35.4
		25000	$2.5 \times 10^6$		
		35000	$3.4 \times 10^6$		
		45000	$4.5 \times 10^6$		
		55000	$5.5 \times 10^6$		
San Fernando	1202	15000	$0.25 \times 10^6$	5.17	32.38
		25000	$0.45 \times 10^6$		
		35000	$0.65 \times 10^6$		
		45000	$0.82 \times 10^6$		
		55000	$1.00 \times 10^6$		

Additionally, Table 3 presents values of the peak lateral displacement for the structural models with the same story mass of 35000 kg applied for all stories. As it can be seen from the table, the peak lateral displacement is equal to 69.2 cm, 59.9 cm, 43.89 cm, 35.4 cm, 33.76 cm and finally, 32.38 cm for the stories stiffness of  $4.45 \times 10^6$  N/m,  $0.9 \times 10^6$  N/m,  $2.00 \times 10^6$  N/m,  $3.4 \times 10^6$  N/m,  $1.00 \times 10^6$  N/m



and finally,  $0.65 \times 10^6$  N/m, respectively. These results indicate that the largest stories stiffness results in the maximum peak lateral displacement and, subsequently, the lowest stories stiffness has demonstrated the minimum peak lateral displacement among all models.

Mass (kg)	Story stiffness (N/m)	Building vibration period (s)	Peak lateral displacement (cm)
35000	$0.65 \times 10^6$	5.17	32.38
	$0.9 \times 10^6$	4.22	59.9
	$1 \times 10^6$	4.11	33.76
	$2 \times 10^6$	2.91	43.89
	$3.4 \times 10^6$	2.23	35.4
	$4.45 \times 10^6$	1.96	69.2

### 3.3. ANN model

In the study, the ANN has been used so as to predict the peak lateral displacement of the multi-story buildings with different properties (height of stories, number of stories, mass of stories, stiffness of stories and building vibration period) exposed to earthquakes with various PGA. The schematic diagram of the ANN model is shown in Figure 3.

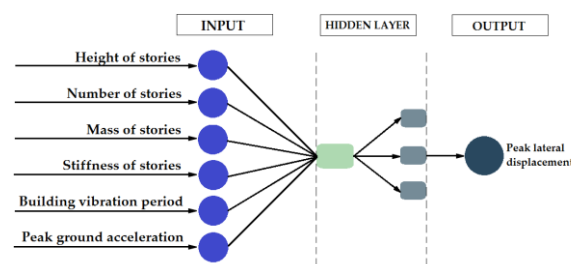


**Fig. 3** Schematic architecture of the ANN model.

The following parameters (independent variables) have been considered to be the input signals:

- height of stories;
- number of stories;
- mass of stories;
- stiffness of stories;
- building vibration period;
- PGA.

The output signal is the predicted peak lateral displacement value of the multi-story building. As a consequence, the created network has the following structure: 6- $n$ -1, so there are six inputs,  $n$  hidden neurons and one output. Different lumped stories mass from 15000 kg to 55000 kg, different stories stiffness from  $0.1 \times 10^6$  N/m to  $5 \times 10^6$  N/m, and also six earthquake records with various PGA values from  $300 \text{ cm/s}^2$  to  $1200 \text{ cm/s}^2$ , have been considered in the investigation using the ANN.

The details of the ANN analysis for a specified set of inputs can be found in a number of other publications (see [39-40], for example). Nevertheless, in order to describe the methodology of the method, it should be mentioned that the input category is generally made by the ANN, and all of them are coordinated to find an iterative procedure between each other and automatically analyzed in the second layer. The learning process is conducted through the internal processing functions. Then, the activation functions and the input signal are processed to obtain the output signal, which is compared with the actual result given by the system wizard (validation process) (see [38]).

In the study described in the present paper, the output has been obtained as the value of the peak lateral displacement of each model with different properties exposed to earthquake records with

various PGA. For this purpose, all analyses (after learning) have informed all inputs to start and create a trend to be evaluated by ANN, and finally, the results of predicted lateral displacement based on all analyses has been predicted. The examples of the results of the ANN analysis are graphically depicted in Figure 4 and compared with the previously calculated peak lateral displacements using numerical simulations. The comparison between the calculated and predicted values confirms the accuracy of the ANN algorithm used.

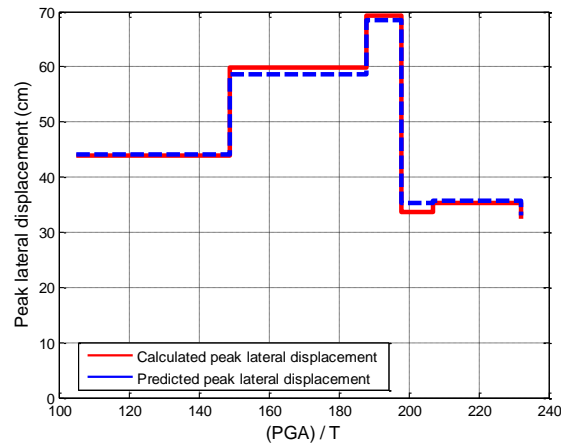
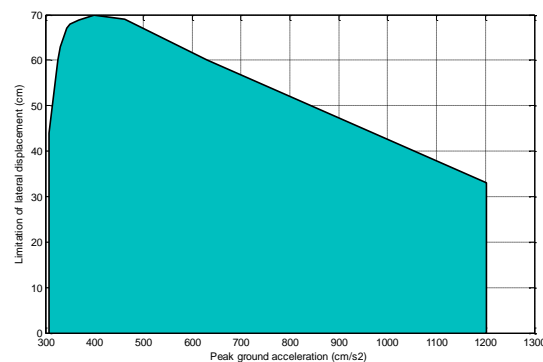


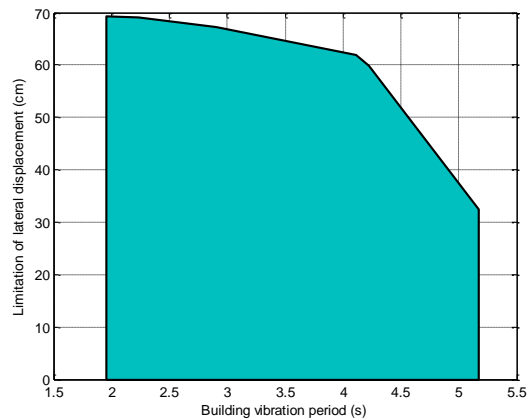
**Fig. 4** Comparison between the calculated and predicted peak lateral displacements.

### 3.3.1. ANN learning and validation process

Using the ANN, with the schematic diagram shown in Figure 3, the peak lateral displacement has been determined for different structural arrangements and earthquake records. Data summarized in Table 3 have been used to start the procedure. Based on all inputs and learned trend of solution to determine the peak lateral displacement, the ANN has been applied to select a value of stories mass, stories stiffness and building vibration period. Then, considering the number and height of stories, the process has been mathematically started to determine the peak lateral displacement. The results of the first stage of the analysis, in the form of the graphical relation between the limitation of the peak lateral displacement and PGA of the ground motion, and also building vibration period, are presented in Figure 5. It can be seen from the figure that the ANN has logically predicted the limitation of the peak lateral displacement for a five-story building with different properties. These results have been applied in further investigation. For example, the five-story building with a value of 2.65 s vibration period has been selected to be exposed to the earthquake record with PGA of 1150  $\text{cm/s}^2$ .



(a)



(b)

**Fig. 5** The limitation of the peak lateral displacement with relation to a) PGA and b) Period. Different dominations have been suggested based on a relation between PGA and building vibration period,  $T$ , as defined by the formula:

$$\alpha = \frac{\text{PGA}}{T} \quad (14)$$

For different ranges of  $\alpha$ , the domination of the peak lateral displacement is presented as follow:

$$\left\{ \begin{array}{l} \alpha < 140 \rightarrow \delta < 50 \quad (\text{cm}) \\ 140 \leq \alpha < 165 \rightarrow \delta < 60 \quad (\text{cm}) \\ 165 \leq \alpha < 190 \rightarrow \delta < 70 \quad (\text{cm}) \\ \alpha \geq 190 \rightarrow \delta < 40 \quad (\text{cm}) \end{array} \right. \quad (15)$$

### 3.3.2. ANN testing process

In order to fully verify the accuracy of the method, the study has been extended for buildings with different values of mass, stiffness of each story and PGA values of earthquake record. For the validation purposes of the process, the stories mass and stories stiffness have been firstly investigated so as to determine the peak lateral displacement. Then, the study has been focused on critical distance between two adjacent buildings so as to prevent their pounding during earthquakes.

In here, five-story model with a lumped stories mass of 25500 kg and stories stiffness of  $3.15 \times 10^6$  N/m has been considered to be exposed to the Kocaeli earthquake record. The building vibration period of the model has been taken as equal to 1.98 s and the PGA of earthquake record as 369 cm/s<sup>2</sup>. Thus, the value of  $\alpha = 186.36$  has been calculated based on equation (14) and the domination of the peak lateral displacement has been assessed as smaller than 70 cm (see equation (15)). The representative example of the results of the analysis in the form of the lateral displacement time history for the Kocaeli earthquake record is shown in Figure 6. As it can be seen from the figure, the peak lateral displacement of 65.48 cm (smaller than 70 cm) has been obtained in this case.

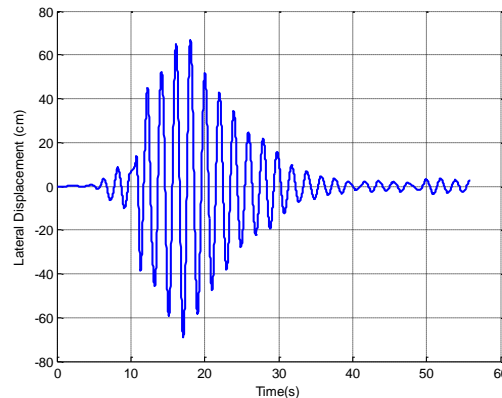
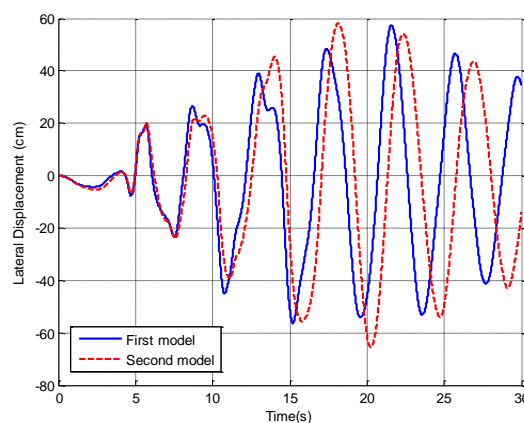
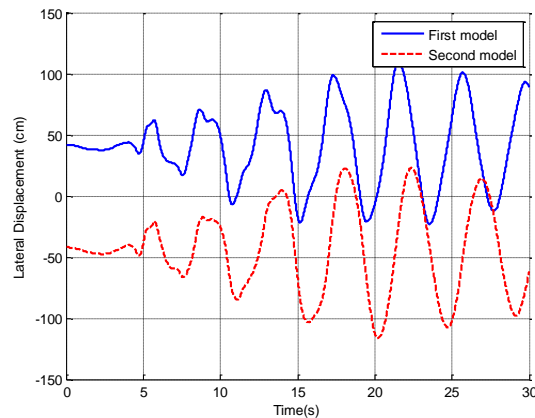


**Fig. 6** The lateral displacement time history under the Kocaeli earthquake record.

The second part of the investigation has been focused on critical distance between two adjacent buildings so as to prevent their pounding during earthquakes. For this challenge, two five-story buildings have been considered to be located close to each other. The first building has stories mass equal to 49530 kg and stories stiffness of  $1.45 \times 10^6$  N/m while the second one has stories mass equal to 22430 kg and the stories stiffness of  $0.55 \times 10^6$  N/m. The vibration periods of two structures are equal to 4.08 s and 4.45 s while the value of  $\alpha$  is 154 and 141, respectively. Therefore, it can be predicted that the domination of the peak lateral displacements for both structures is smaller than 60 cm (see equation (15)). The examples of the results obtained for the Loma Prieta earthquake record (PGA=631  $\text{cm/s}^2$ ) are presented in Figure 9. It can be seen from Figure 9a that the peak lateral displacement is equal to 58.4 cm and 56.5 cm (smaller than 60 cm) for the first and the second building, respectively. Having the peak lateral displacement of both models and using equation (2), sufficient separation distance between two five-story buildings has been calculated as equal to 81.3 cm. Figure 7b shows that the value is large enough to prevent pounding under the Loma Prieta earthquake.



(a)

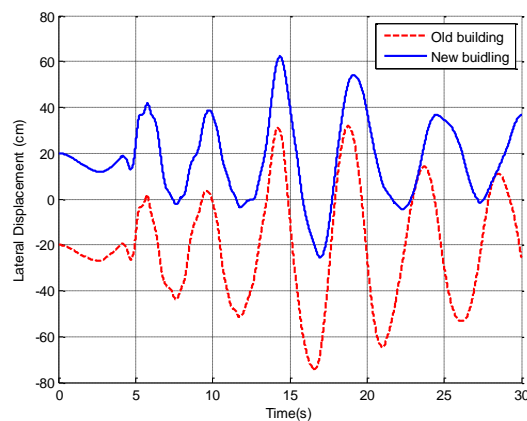


(b)

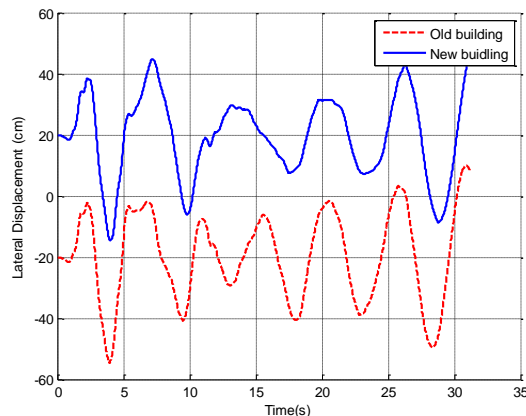
**Fig. 7** The lateral displacement time histories of buildings under the Loma Prieta earthquake record: a) without separation; b) with separation - seismic gap of 82 cm.

It has been assumed in the final stage of the investigation that close to the existing (old) five-story building with stories mass of 35500 kg and stories stiffness of  $0.58 \times 10^6$  N/m, a new structure will be constructed at the distance of 40 cm. The old building vibration period has been calculated as equal to 5.46 s. Based on the process of the ANN, the limitation of the peak lateral displacement of this building has been determined as equal to 37.25 cm. Moreover, the vibration period of new building has been calculated as equal to 5.2 s which can be organized by stories mass of 34000 kg and stories stiffness of  $0.67 \times 10^6$  N/m.

In order to confirm the process of using the ANN and verify the results of the calculated stories mass and stories stiffness for a new building, two buildings have been considered to be exposed to different seismic excitations. The representative results of the analysis obtained for the Loma Prieta and El Centro earthquake records are shown in Figure 8a and Figure 8b, respectively. As it can be seen from the figures, the separation distance of 40 cm is large enough to prevent structural pounding for both earthquakes considered.



(a)



(b)

**Fig. 8** The lateral displacement time histories of buildings separated by the seismic gap of 40 cm: a) under the Loma Prieta earthquake; b) under the El Centro.

#### 4. Concluding remarks

The process of predicting the peak lateral displacement of the multi-story building under earthquake excitations using the ANN has been proposed in this paper. Firstly, the investigation on determination of the peak lateral displacement has been conducted for the model of five-story building. For this purpose the lumped-mass structural model with various stories mass and stories stiffness has been analyzed under six earthquake records with different PGA. Then, the ANN has been applied so as to determine the limitation of the peak lateral structural displacement. The input signals have been assumed to be the structural parameters (height of stories, number of stories, mass of stories, stiffness of stories, building vibration period) and the PGA of ground motion. The output signal has been predicted in the form of the peak lateral displacement of the building. The created algorithm, as well as the validation and testing of the ANN model, have been presented. Then, the study has been focused on critical distance between two adjacent buildings so as to prevent their pounding during earthquakes.

It should be underlined that the proposed ANN has logically predicted the limitation of the peak lateral displacement for the five-story building with different properties. The results of the study clearly indicate that the ANN is also capable to properly predict the peak lateral displacements for two buildings so as to prevent their pounding under different earthquakes. Subsequently, calculation of critical distance can also be optimized to save the land and provide the safety space between two adjacent buildings prone to seismic excitations.

#### 5. References

- [1] Miari, M.; Choong, K.K.; Jankowski, R. Seismic pounding between adjacent buildings: Identification of parameters, soil interaction issues and mitigation measures. *Soil Dynamics and Earthquake Engineering* 2019, 121, 135–150. DOI: 10.1016/j.soildyn.2019.02.024.
- [2] Kazemi, F.; Miari, M.; Jankowski, R. Investigating the effects of structural pounding on the seismic performance of adjacent RC and steel MRFs. *Bulletin of Earthquake Engineering* 2021, 19(1), 317–343. DOI: 10.1007/s10518-020-00985-y.
- [3] Anagnostopoulos, S.A. Pounding of building in series during earthquakes. *Earthquake Engineering and Structural Dynamics* 1988, 16(3), 443–456.
- [4] Polycarpou, P.C.; Komodromos, P. Numerical investigation of potential mitigation measures for pounding of seismically isolated building. *Earthquakes and Structures* 2011, 2, 1–24.
- [5] Favvata, M.J. Minimum required separation gap for adjacent RC frames with potential inter-story seismic pounding. *Engineering Structures* 2017, 152, 643–659.

- [6] Rezaei, H.; Moayyedi, S.A.; Jankowski, R. Probabilistic seismic assessment of RC box-girder highway bridges with unequal-height piers subjected to earthquake-induced pounding. *Bulletin of Earthquake Engineering* 2020, 18(4), 1547–1578.
- [7] Naderpour, H.; Barros, R.C.; Khatami, S.M. Suggestion of an equation of motion to calculate the damping ratio during earthquake based on a cyclic procedure. *Journal of Theoretical and Applied Mechanics* 2016, 54(3), 963–973. DOI: 10.15632/jtam-pl.54.3.963.
- [8] Naderpour, H.; Barros, R.C.; Khatami, S.M.; Jankowski, R. Numerical study on pounding between two adjacent buildings under earthquake excitation. *Shock and Vibration* 2016, 2016, 1504783. DOI: 10.1155/2016/1504783.
- [9] Lopez-Garcia, D. Separation between adjacent non-linear structures for prevention of seismic pounding. In *Proceedings of 13th World Conference on Earthquake Engineering*, Vancouver, Canada, 2004.
- [10] Lopez-Garcia, D.; Soong, T.T. Evaluation of current criteria in predicting the separation necessary to prevent seismic pounding between nonlinear hysteretic structural systems. *Engineering Structures* 2009, 31, 1217–1229. DOI: 10.1016/j.engstruct.2009.01.016.
- [11] IBC: International Building Code, International Code Council Inc., Country Club Hills, Illinois, USA, 2009.
- [12] Eurocode 8: Design of Structures for Earthquake Resistance; European Committee for Standardization: Brussels, Belgium, 2003.
- [13] Building & Housing Research Center: Iranian code of practice for seismic resistant design of buildings, Permanent Committee of Revising the Code of Practice for Seismic Resistant Design of Buildings, BHRC Publication No. 465, 2017, pp. 94.
- [14] Kiureghian, A.D. A response spectrum method for random vibration analysis of MDF systems. *Earthquake Engineering and Structural Dynamics* 1981, 9, 419–435. DOI:10.1002/eqe.4290090503.
- [15] Jeng, V.; Kasai, K.; Maison, B.F. A Spectral difference method to estimate building separations to avoid pounding. *Earthquake Spectra* 1992, 8(2), 201–223. DOI: 10.1193/1.1585679.
- [16] Soltysik, B.; Jankowski, R. Non-linear strain rate analysis of earthquake-induced pounding between steel buildings. *International Journal of Earth Sciences and Engineering* 2013, 6(3), 429–433.
- [17] Elwardany, H.; Seleemah, A.; Jankowski, R.; El-Khoriby, S. Influence of soil-structure interaction on seismic pounding between steel frame buildings considering the effect of infill panels. *Bulletin of Earthquake Engineering* 2019, 17(11), 6165–6202.
- [18] Filiatrault, A.; Wagner, P.; Cherry, S. Analytical prediction of experimental building pounding. *Earthquake Engineering and Structural dynamics* 1995, 24(8), 1131–1154. 1995. DOI: 10.1002/eqe.4290240807.
- [19] Penzien, J. Evaluation of building separation distance required to prevent pounding during strong earthquakes. *Earthquake Engineering and Structural Dynamics* 1997, 26(8), 849–858. DOI: doi.org/10.1002/(SICI)1096-9845(199708)26:8<849::AID-EQE680>3.0.CO;2-M.
- [20] Rahman, A.M.; Carr, A.J.; Moss, P.J. Structural pounding of adjacent multi-storey structures considering soil flexibility effects. In *Proceedings of the 12th World Conference on Earthquake Engineering*, Auckland, New Zealand, 30 January–4 February 2000.
- [21] Naderpour, H.; Barros, R.C.; Khatami, S.M. Prediction of critical distance between two MDOF systems subjected to seismic excitation in terms of artificial neural networks. *Period. Polytech. Civ. Eng.* 2017, 61, 516–529. DOI: 10.3311/PPci.9618.
- [22] Khatami, S.M; Naderpour, H.; Barros, R.C.; Jankowski, R. Verification of formulas for periods of adjacent buildings used to assess minimum separation gap preventing structural pounding during earthquakes. *Advances in Civil Engineering* 2019, 2019, 9714939. DOI: 10.1155/2019/9714939.
- [23] Goetz, T. *The Decision Tree: How to Make Better Choices and Take Control of Your Health*; Rodale Books: Emmaus, PA, USA, 2010.
- [24] Jankowski, R.; Walukiewicz, H. Modeling of two-dimensional random fields. *Probabilistic Eng. Mech.* 1997, 12, 115–121. DOI: 10.1016/S0266-8920(96)00040-9.

- [25] Siemaszko, A.; Jakubczyk-Gałczyńska, A.; Jankowski, R. The idea of using Bayesian networks in forecasting impact of traffic-induced vibrations transmitted through the ground on residential buildings. *Geosciences* 2019, 9, 339. DOI: 10.3390/geosciences9080339.
- [26] Kamgar, R.; Naderpour, H.; Komeleh, H.E.; Jakubczyk-Gałczyńska, A.; Jankowski, R. A proposed soft computing model for ultimate strength estimation of FRP-confined concrete cylinders. *Applied Sciences* 2020, 10, 1769. DOI: 10.3390/app10051769.
- [27] Khatami, S.M.; Naderpour, H.; Razavi, S.M.N.; Barros, R.C., Sołtysik, B.; Jankowski, R. An ANN-based approach for prediction of sufficient seismic gap between adjacent buildings prone to earthquake-induced pounding. *Applied Sciences* 2020, 10(10), 3591. DOI: 10.3390/app10103591.
- [28] Jakubczyk-Gałczyńska A.; Jankowski R. (2020) A proposed machine learning model for forecasting impact of traffic-induced vibrations on buildings. *Lecture Notes in Computer Science* 2020, 12139, 444-451. DOI: 10.1007/978-3-030-50420-5\_33
- [29] Naderpour, H.; Kheyroddin, A.; Amiri, G.G. Prediction of FRP-confined compressive strength of concrete using artificial neural networks. *Compos. Struct.* 2010, 92, 2817–2829. DOI: 10.1016/j.compstruct.2010.04.008
- [30] Naderpour, H.; Rafiean, A.H.; Fakharian, P. Compressive strength prediction of environmentally friendly concrete using artificial neural networks. *J. Build. Eng.* 2018, 16, 213–219. DOI: 10.1016/j.job.2018.01.007.
- [31] Ahmadi, M.; Naderpour, H.; Kheyroddin, A. Utilization of artificial neural networks to prediction of the capacity of CCFT short columns subject to short term axial load. *Arch. Civ. Mech. Eng.* 2014, 14, 510–517. DOI: 10.1016/j.acme.2014.01.006.
- [32] Chopra, A.K.; Chintanapakdee, C. Inelastic deformation ratios for design and evaluation of structures: Single-degree-of-freedom bilinear systems. *J. Struct. Eng.* 2004, 130, 1309–1319. DOI: 10.1061/(ASCE) 0733-9445(2004)130:9(1309).
- [33] Iervolino, I.; Chioccarelli, E.; Baltzopoulos, G. Inelastic displacement ratio of near-source pulse-like ground motions. *Earthq. Eng. Struct. Dyn.* 2012, 41, 2351–2357. DOI: 10.1002/eqe.2167.
- [34] Anajafi, H.; Poursadr, K.; Roohi, M.; Santini-Bell, E. Effectiveness of seismic isolation for long-period structures subject to far-field and near-field excitations. *Front. Built Env.* 2020, 6, 24. DOI: 10.3389/ fbuil.2020.00024.
- [35] Léger, P.; Dussault, S. Seismic-energy dissipation in MDOF structures. *J. Struct. Eng.* 1992, 118, 1251–1269. DOI: 10.1061/(ASCE)0733-9445(1992)118:5(1251).
- [36] Anajafi, H.; Medina, R.A.; Santini-Bell, E. Effects of the improper modeling of viscous damping on the first-mode and higher-mode dominated responses of base-isolated buildings. *Earthq. Eng. Struct. Dyn.* 2020, 49, 51–73. DOI: <https://doi.org/10.1002/eqe.3223>.
- [37] Charney, F.A. Unintended consequences of modeling damping in structures. *J. Struct. Eng.* 2008, 134, 581–592. DOI: 10.1061/(ASCE)0733-9445(2008)134:4(581).
- [38] Jakubczyk-Gałczyńska, A. Predicting the impact of traffic-induced vibrations on buildings using artificial neural networks. *MATEC Web of Conferences* 2018, 219, 04004. DOI: 10.1051/mateconf/201821904004.
- [39] Rojas, R. *Neural Networks: A Systematic Introduction*; Springer Science & Business Media: Berlin/Heidelberg, Germany, 2013.
- [40] Hüskén, M.; Jin, Y.; Sendhoff, B. Structure optimization of neural networks for evolutionary design optimization. *Soft Comput.* 2005, 9, 21–28. DOI: 10.1007/s00500-003-0330-y.